Supporting Information

Synthesis of *P*-Triazole Dithienophospholes and a Cyclodextrin-based Sensor via Click Chemistry

Xiaoming He, Ping Zhang, Jian-Bin Lin, Huy V. Huynh, Sandra E. Navarro Muñoz, Chang-Chun Ling and Thomas Baumgartner*

Department of Chemistry & Centre for Advanced Solar Materials, University of Calgary, 2500 University Drive, NW, Calgary, Alberta T2N 1N4, Canada

thomas.baumgartner@ucalgary.ca

Experimental section

Materials and Methods. All chemical reagents were purchased from commercial sources (Aldrich, Alfa Aesar, Strem) and were, unless otherwise noted, used without further purification Solvents were dried using an MBraun solvent purification system prior to use. Phosphole oxide **A**,[S1] azidobenzene,[S2] 1-azido-4-methoxybenzene,[S3] 1-azido-2,3,4,5,6-pentafluorobenzene,[S3] cyclodextrin azide[S4] were prepared according to reported procedures. All reactions and manipulations were carried out under a dry nitrogen atmosphere employing standard Schlenk techniques. $^{31}P\{^{1}H\}$ NMR, ^{1}H NMR, and $^{13}C\{^{1}H\}$ NMR were recorded on Bruker Avance (-II,-III) 400 MHz spectrometers. Chemical shifts were referenced to external 85% H_3PO_4 (^{31}P) or residual non-deuterated solvent peaks (^{1}H, ^{13}C). Mass spectra were run on a Finnigan SSQ 7000 spectrometer or a Bruker Daltonics AutoFlex III system. All photophysical experiments were carried out on a Jasco FP-6600 spectrofluorometer and UV−vis−NIR Cary 5000 spectrophotometer. Theoretical calculations have been carried out at the B3LYP/6-31G(d) level using the GAUSSIAN 09 suite of programs.[S5] Crystal data and details of the data collection are provided in Table S1 and the corresponding CIF files in the Supporting Information. Diffraction data were collected on a Nonius Kappa CCD diffractometer, using Mo Kα radiation (λ) 0.71073 Å (graphite monochromator). The structures were solved by direct methods (SHELXTL) and refined on F^2 by full-matrix least-squares techniques. CCDC-956580 (**1**), -956579 (**3**), contain the supplementary crystallographic data for this paper. These data can be obtained free of charge from The Cambridge Crystallographic Data Centre via www.ccdc.cam.ac.uk/data_request/cif.

Synthesis of 1-3: Click-phosphole oxide (**A**, 0.2 mmol), azide (0.3 mmol), CuI (8 mg, 20 %) and DIPEA (104 mg, 0.8 mmol) were mixed in THF (4 mL) under the atmosphere of N_2, and stirred for 24 h at room temperature. After removal of the volatiles, the product was purified by chromatography using CH_2Cl_2-CH_3OH (100:5). Yield: 80-90%.

1: ^{31}P NMR (162 MHz, $CDCl_3$, δ): 6.6; ^{1}H NMR (400 MHz, $CDCl_3$, δ): 8.56 (s, 1 H; triazole); 7.72 (m, 2 H; Ph), 7.55 (m, 2 H; Ph), 7.48 (m, 1 H; Ph), 7.32 (dd, J_{HH} = 4.8 Hz, J_{HP} = 3.6 Hz, 2 H; thiophene), 7.26 (dd, J_{HH} = 4.8 Hz, J_{HP} = 2.8 Hz, 2 H; thiophene); ^{13}C NMR (100.6 MHz, $CDCl_3$, δ): 146.6 (d, J_{CP} = 26.7 Hz), 140.1 (d, J_{CP} = 143.7 Hz), 137.2 (d, J_{CP} = 120.5 Hz), 136.4 (s), 130.0 (s), 129.5 (s), 129.2 (d, J_{CP} = 27.5 Hz), 128.6 (d, J_{CP} = 15.9 Hz), 126.1 (d, J_{CP} = 14.8 Hz), 120.9 (s); HRMS (EI, 70 eV) *m/z* = 355.0003 $[M]^+$ (calcd. 354.9991); Melting point T_m = 234-235 °C.

2: ^{31}P NMR (162 MHz, $CDCl_3$, δ): 4.9; ^{1}H NMR (400 MHz, $CDCl_3$, δ): 8.43 (s, 1 H; triazole), 7.65 (d, J_{HH} = 9.2 Hz, 2H; -C_6H_4), 7.42 (dd, J_{HH} = 4.8 Hz, J_{HP} = 3.6 Hz, 2H; thiophene), 7.33 (dd, J_{HH} = 4.8 Hz, J_{HP} = 2.4 Hz, 2H; thiophene), 7.08 (d, J_{HH} = 9.2 Hz, 2H; -C_6H_4), 3.90 (s, 3 H; -OCH_3); ^{13}C NMR (100.6 MHz, $CDCl_3$, δ): 160.4 (s), 146.2 (d, J_{CP} = 26.3 Hz), 140.1 (d, J_{CP} = 143.7 Hz), 137.8 (d, J_{CP} = 119.2 Hz), 129.8 (s), 128.9 (d, J_{CP} = 28.2 Hz), 128.7 (d, J_{CP} = 15.6 Hz), 125.8 (d, J_{CP} = 14.6 Hz), 122.6 (s), 114.9 (s), 55.7 (s); HRMS (EI, 70 eV) *m/z* = 385.0109 $[M]^+$ (calcd. 385.0098); Melting point T_m = 242-244 °C.

3: ^{31}P NMR (162 MHz, $CDCl_3$, δ): 4.0; ^{1}H NMR (400 MHz, $CDCl_3$, δ): 8.44 (s, 1 H; triazole), 7.43 (dd, J_{HH} = 4.8 Hz, J_{HP} = 3.6 Hz, 2H; thiophene), 7.34 (dd, J_{HH} = 4.8 Hz, J_{HP} = 2.8 Hz, 2H; thiophene); ^{19}F NMR: -147.6 (m), -151.7 (m), -161.7 (m); ^{13}C NMR (100.6 MHz, $CDCl_3$, δ): 146.6 (d, J_{CP} = 26.8 Hz), 143.8 (m), 140.9 (d, J_{CP} = 140.7 Hz), 141.2 (m), 139.4 (m), 137.2 (d, J_{CP} = 120.4 Hz), 137.0 (m), 133.3 (d, J_{CP} = 27.0 Hz), 129.0 (d, J_{CP} = 15.8 Hz), 125.9 (d, J_{CP} = 14.7 Hz); HRMS (EI, 70 eV) *m/z* = 444.9532 $[M]^+$ (calcd. 444.9513); Melting point T_m = 212-213 °C.

Synthesis of 4: To a solution of mono-6-azido-6-deoxy-β-cyclodextrin (100 mg, 86 μmol), click-phosphole oxide (**A**, 30 mg, 127 μmol) in anhydrous DMF (1.5 mL) was added CuI (10 mg) and DIPEA (20 μL). The reaction flask was wrapped with tin foil and stirred at RT for 36 h at room temperature. The solution was concentrated under reduced procedure, and the residue was purified by reverse-phase chromatography on C18 silica gel using a gradient of MeOH-H_2O (0→90%) as eluent to afford compound **4** which was lyophilized (61 mg, yield: 51%). ^{31}P NMR (162 MHz, D_2O, δ): 9.2; ^{1}H NMR (400 MHz, D_2O, δ): 8.50 (s, 1H, triazole), 7.59 – 7.51 (dd, J_{HH} = 4.4 Hz, J_{HP} = 4.2 Hz, 2H; thiophene), 7.33 – 7.25 (m, 2H; thiophene), 5.11 – 4.93 (m, 6H; 5 × H-1_Glu + H-6a_Glu), 4.87 (d, *J* = 3.7 Hz, 1H; H-1_Glu), 4.83 (d, *J* = 3.6 Hz, 1H; H-1_Glu), 4.61 (overlapped with HDO, *J* = 14.5, 9.6 Hz, 1H; H-6b_Glu), 4.12 (ddd, *J* = 9.8, 9.8, ~ 1 Hz, 1H; H-5_Glu), 3.92 – 3.35 (m, 36H; 7 × H-2 + 7 × H-3 + 7 × H-4 + 5 × H-5 + 5 × H-6a + 5 × H-6b), 3.20 (m, 1H; H-5_Glu), 2.56 (dd, *J* = 11.3, ~1 Hz, 1H; H-6a), 2.38 (dd, *J* = 12.2, 1.8 Hz, 1H; H-6b_Glu). ^{13}C NMR (100 MHz, D_2O, selected, due to poor resolution of spectrum δ): 130.78, 130.62, 125.47, 125.31, 125.16, 102.04, 102.00, 101.95, 101.93, 101.82, 101.79, 101.27, 82.98, 81.24, 81.17, 81.12, 81.08, 81.03, 80.19, 73.11, 73.02, 72.81, 72.67, 72.01, 71.94, 71.82, 71.71, 71.47, 70.37, 60.19, 60.01, 58.68, 51.69; HRMS (ESI QTOF) *m/z* = 1418.3114 $[M + Na]^+$ (calcd. 1418.3180).

Reference

(S1) He. X. M.; Lin, J. B.; Kan, W. H.; Dong, P.; Trudel, S.; Baumgartner, T. *Adv. Funct. Mater.* **2013**, DOI: 10.1002/adfm.201302294.

(S2) Berger, O.; Kaniti, A.; van Ba, C. T.; Vial, H.; Ward, S. A.; Biagini, G. A.; Bray, P. G.; O'Neill, P. M. *ChemMedChem* **2011**, *6*, 2094-2108.

(S3) Kloss, F.; Köhn, U.; Jahn, B. O.; Hager, M. D.; Görls, H.; Schubert, U. S. *Chem. Asian J.* **2011**, *6*, 2816-2824.

(S4) Hocquelet, C.; Blu, J.; Jankowski, C. K.; Arseneau, S.; Buisson, D.; Mauclaire, L. *Tetrahedron* **2006**, *62*, 11963-11971.

(S5) Ref. 17.

Table S1. Crystal data and structure refinement for **1** and **3.**

Complex	**1**	**3**
Compound	$C_{16}H_{10}N_3OPS_2$	$C_{16}H_5F_5N_3OPS_2$x0.17(CH_3OH)
Formula	$C_{16}H_{10}N_3OPS_2$	$C_{16.17}H_{5.68}F_5N_3O_{1.17}PS_2$
Formula weight	355.36	450.66
Crystal system	Triclinic	Trigonal
Space group	*P*-1	*R*-3
a/Å	11.4280(4)	35.0181(11)
b/Å	11.7430(4)	35.0181(11)
c/Å	12.2150(4)	8.0290(2)
α/°	103.705(2)	90
β/°	104.420(2)	90
γ/°	93.6210(19)	120
V/Å ^{3}	1529.34(9)	8526.6(4)
Z	4	18
D_c/g cm^{-3}	1.543	1.580
μ/mm^{-1}	0.459	0.426
temperature / K	173(2)	173(2)
reflns coll.	11112	19619
unique reflns	5954	3723
R_{int}	0.0228	0.0607
R_1 [$I > 2\sigma(I)$][a]	0.0462	0.0620
wR_2 [$I > 2\sigma(I)$][b]	0.1242	0.1947
R_1 (all data)	0.0573	0.0803
wR_2 (all data)	0.1433	0.2202
GOF	1.007	1.007

$R_1 = \sum||F_o| - |F_c||/\sum|F_o|$. $wR_2 = [\sum w(F_o^2 - F_c^2)^2/\sum w(F_o^2)^2]^{1/2}$.

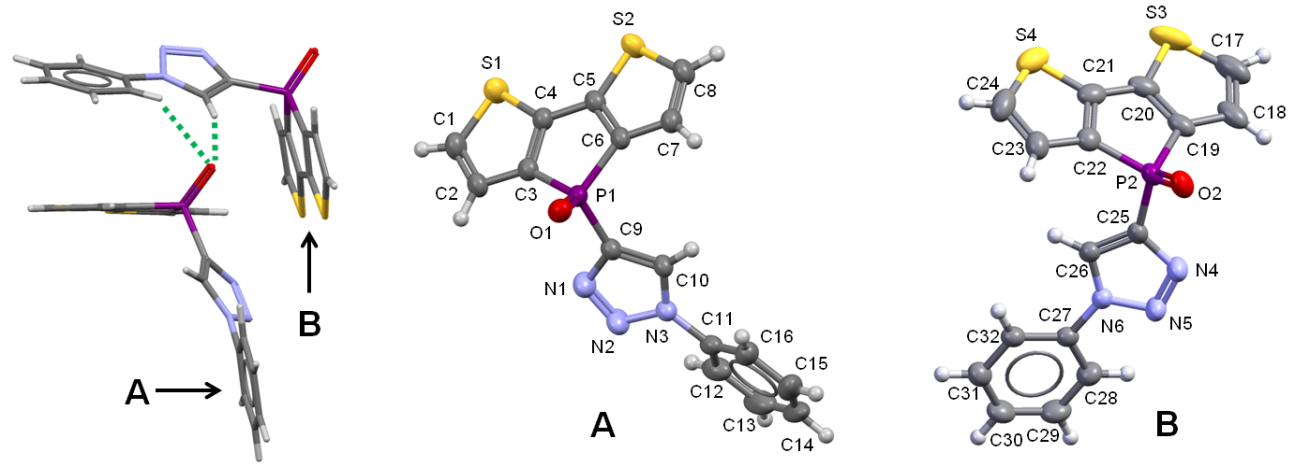

Figure S1. Molecular structures of **1** in the solid state (50% probability level), containing two independent molecules A and B.

Selected bond lengths [Å] and angles [°]:

For **1(A)**: P1-C3, 1.790(2); P1-C6, 1.790(3); P1-C9, 1.774(2); P1-O1, 1.471(2); N1-N2, 1.299(3); N2-N3, 1.349(3); N3-C10, 1.339(3); C10-C9, 1.361(3); C1-C2, 1.349(5); C2-C3, 1.409(3); C3-C4, 1.362(4); C4-C5, 1.454(3); C5-C6, 1.373(3); C6-C7, 1.403(4); C7-C8, 1.349(6);

O1-P1-C3, 117.3(1); O1-P1-C6, 118.9(1); O1-P1-C9, 113.0(1); C3-P1-C9, 107.4(1); C3-P1-C6, 92.3(1); C6-P1-C9, 105.6(1);

Dihedral angle between triazole and Ph: 36.12°

For **1(B)**: P2-C19, 1.790(2); P2-C22, 1.786(3); P2-C25, 1.773(3); P2-O2, 1.473(2); N4-N5, 1.298(4); N5-N6, 1.355(3); N6-C26, 1.343(3); C26-C25, 1.363(3); C17-C18, 1.347(5); C18-C19, 1.412(4); C19-C20, 1.359(5); C20-C21, 1.445(5); C21-C22, 1.376(4); C22-C23, 1.411(5); C23-C24, 1.361(5);

O2-P2-C19, 115.3(1); O2-P2-C22, 120.2(1); O2-P2-C25, 114.3(1); C19-P2-C25, 108.3(1); C19-P2-C22, 92.2(1); C22-P2-C25, 103.9(1);

Dihedral angle between triazole and Ph: 21.50°

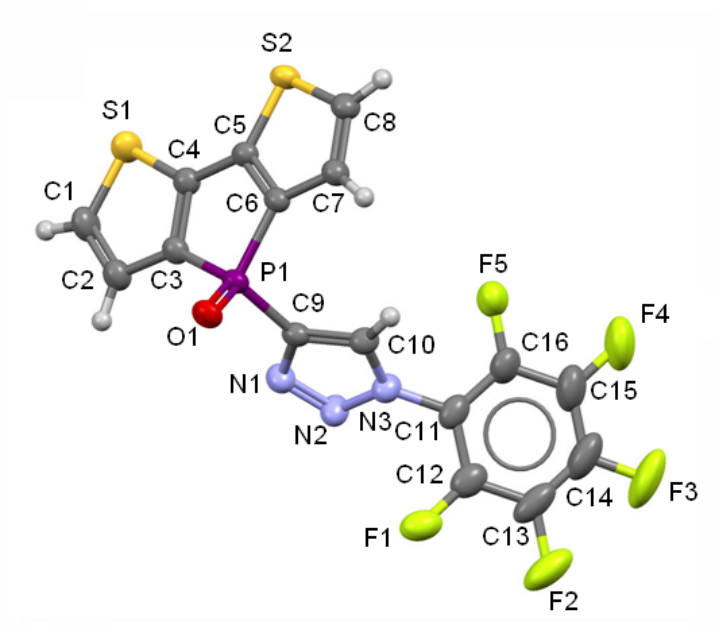

Figure S2. Molecular structures of **3** in the solid state (50% probability level).

Selected bond lengths [Å] and angles [°]: P1-C3, 1.782(4); P1-C6, 1.794(4); P1-C9, 1.775(4); P1-O1, 1.475(4); N1-N2, 1.284(5); N2-N3, 1.365(5); N3-C10, 1.337(6); C10-C9, 1.364(5); C1-C2, 1.353(6); C2-C3, 1.411(6); C3-C4, 1.378(6); C4-C5, 1.450(6); C5-C6, 1.363(5); C6-C7, 1.409(6); C7-C8, 1.352(6); F1-C12, 1.322(6); F2-C13, 1.333(7); F3-C14, 1.325(6); F4-C15, 1.321(7); F5-C16, 1.325(5);

O1-P1-C3,116.9 (2); O1-P1-C6, 119.2(2); O1-P1-C9, 111.6(6); C3-P1-C9, 109.5(2); C3-P1-C6, 93.0(2); C6-P1-C9, 104.8(2);

Dihedral angle between triazole and C_6F_5: 56.61°

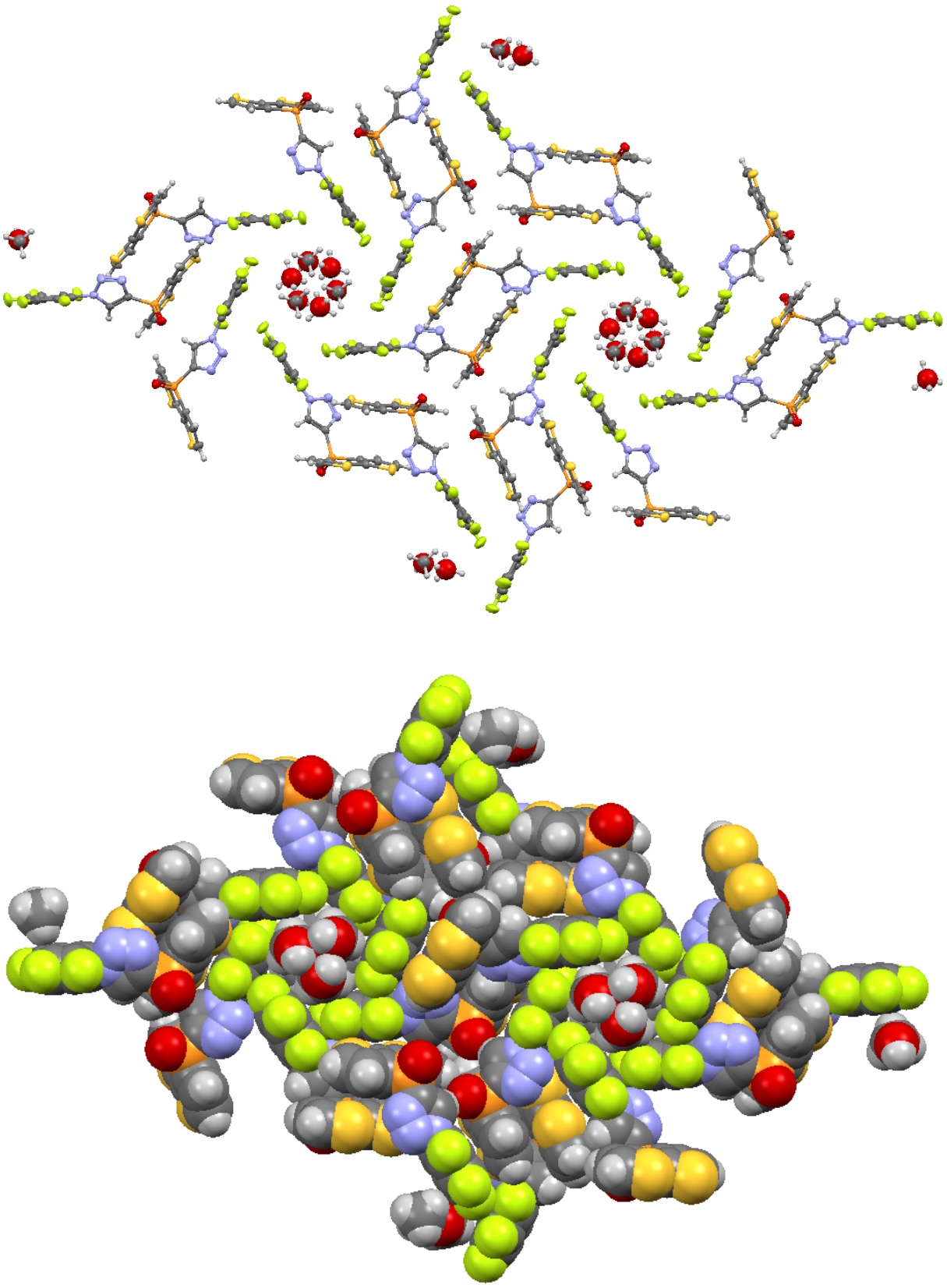

Figure S3. Supramolecular organization of **3** in the solid state

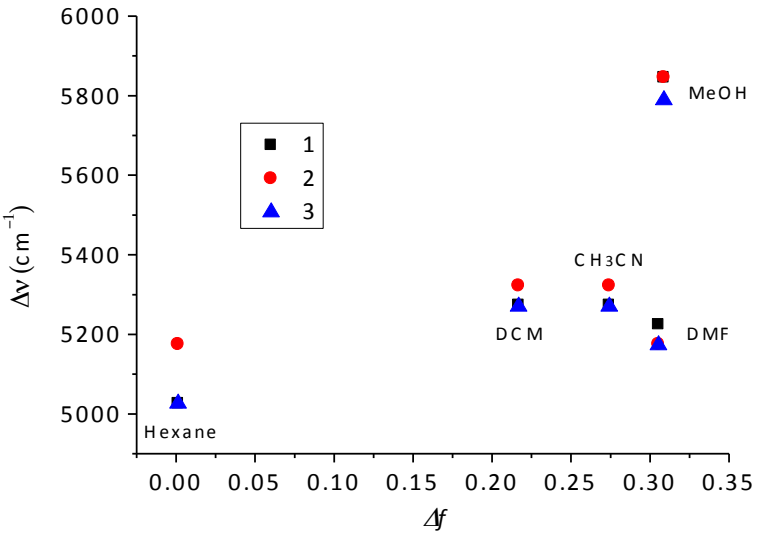

Figure S4. Lippert−Mataga plot for **1-3** in different solvents.

$\Delta\nu$: Stokes shift;
Δf : Lippert solvent parameter $\Delta f = f(\varepsilon) - f(n^2)$;
$f(\varepsilon) = (\varepsilon - 1) / (2\varepsilon + 1)$ and $f(n^2) = (n^2 - 1) / (2n^2 + 1)$, where ε is the dielectric constant and n the refractive index of the corresponding solvent.

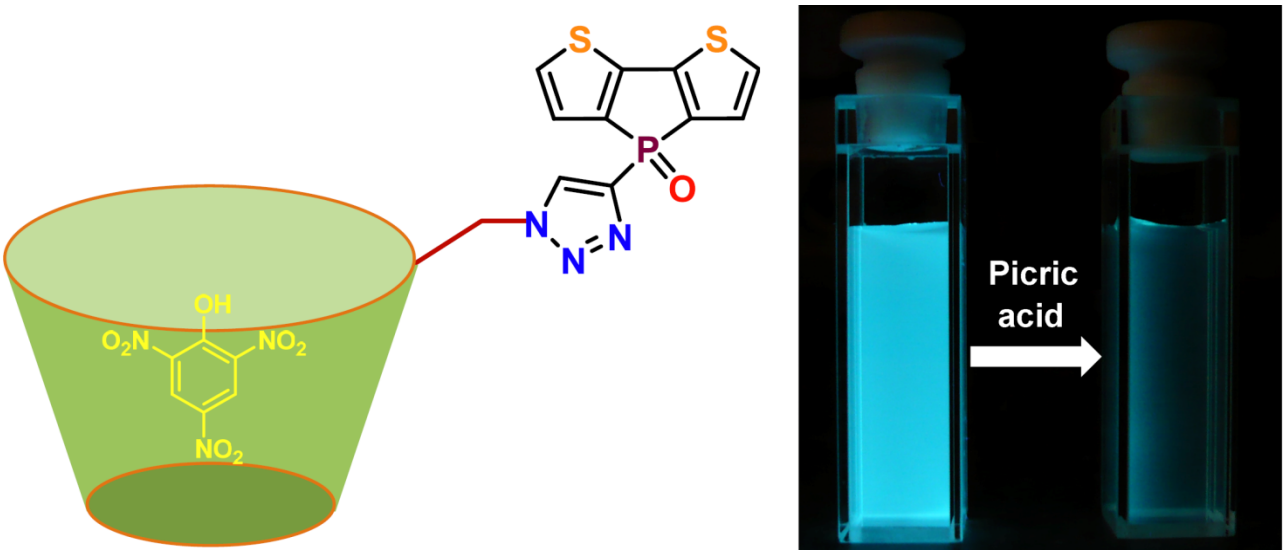

Figure S5. Illustration of the binding mode of **4** for picric acid (left), and the fluorescence response (right)

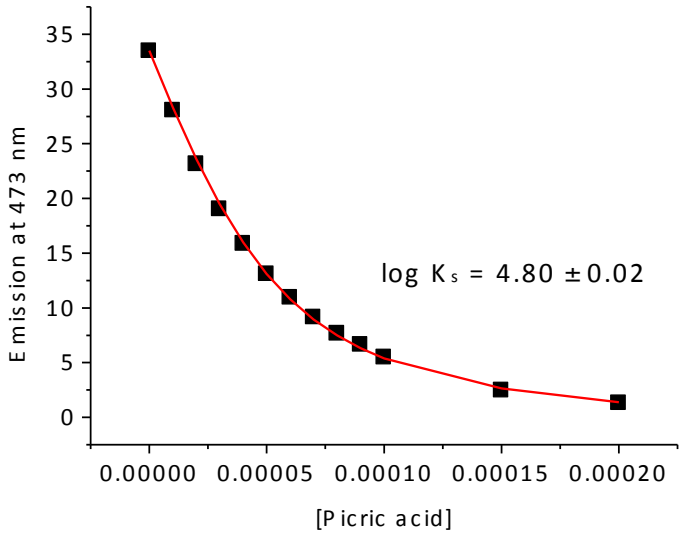

Figure S6. Plot of emission intensity at 473 nm as a function of picric acid concentration and its theoretical fit for the 1:1 binding of complex **4** with picric acid

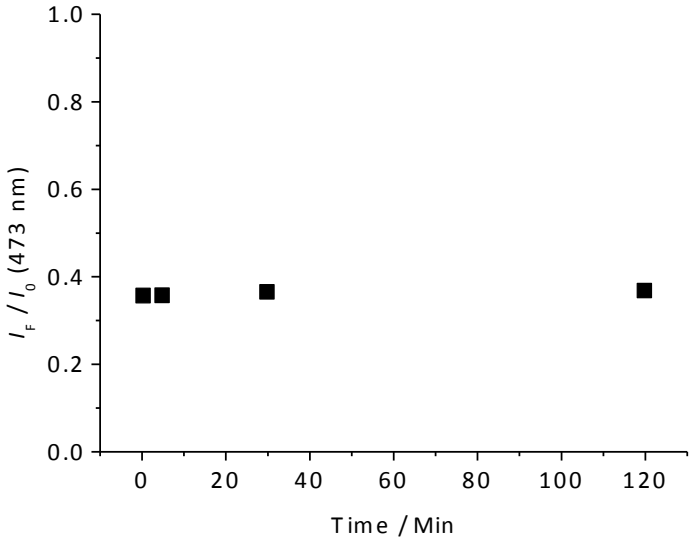

Figure S7. Plot of the ratio (I_F / I_0) of emission intensity at 473 nm as a function of time in the presence (I_F) and absence (I_0) of 1 eq. of picric acid

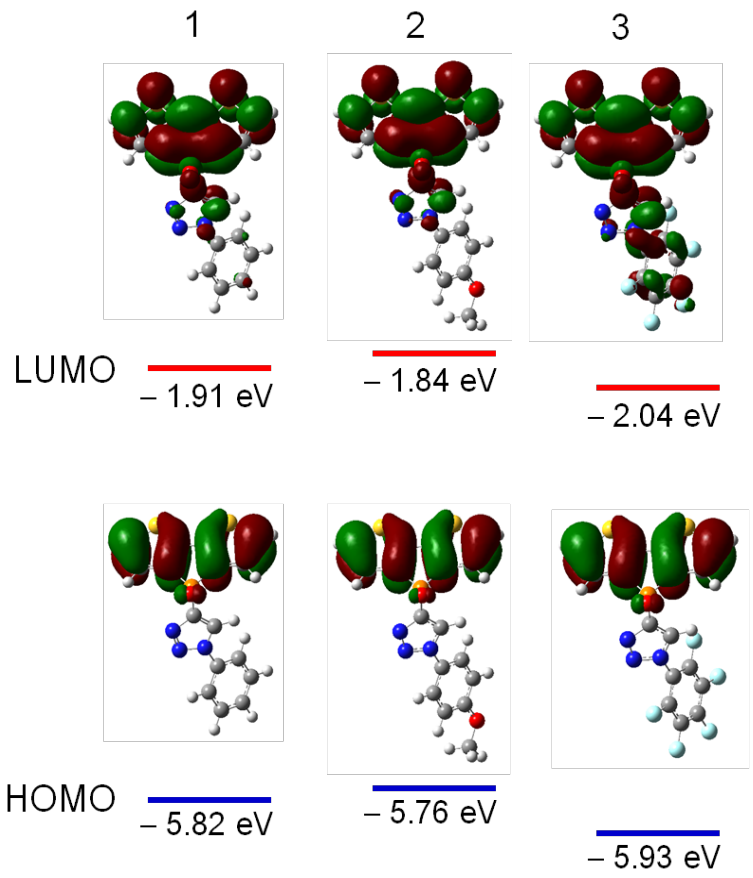

Figure S8. HOMO (bottom) and LUMO (top) orbital diagrams of **1-3**, as well as their energies calculated at B3LYP/6-31G(d) level

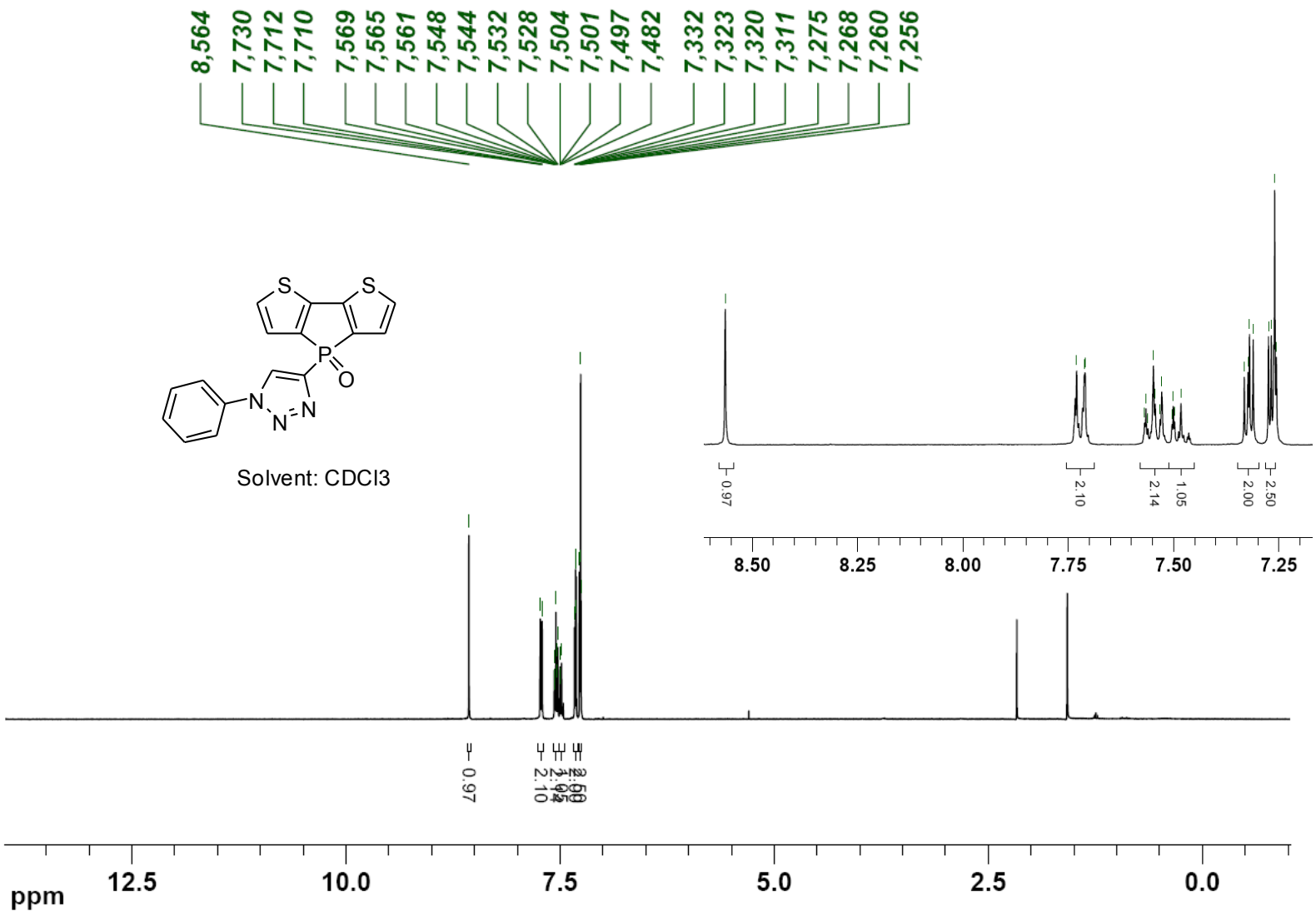

^{1}H NMR of **1** in $CDCl_3$

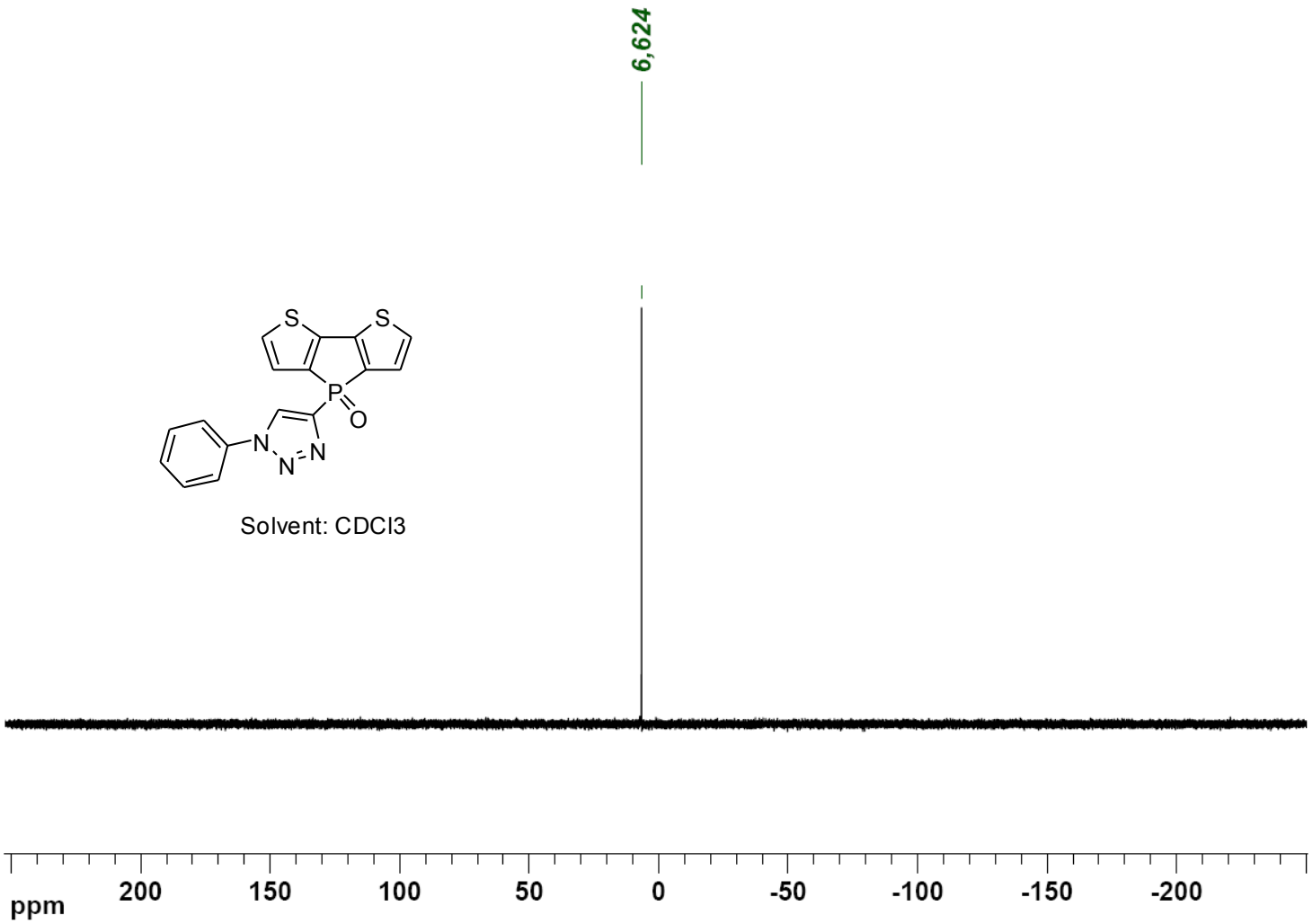

^{31}P NMR of **1** in $CDCl_3$

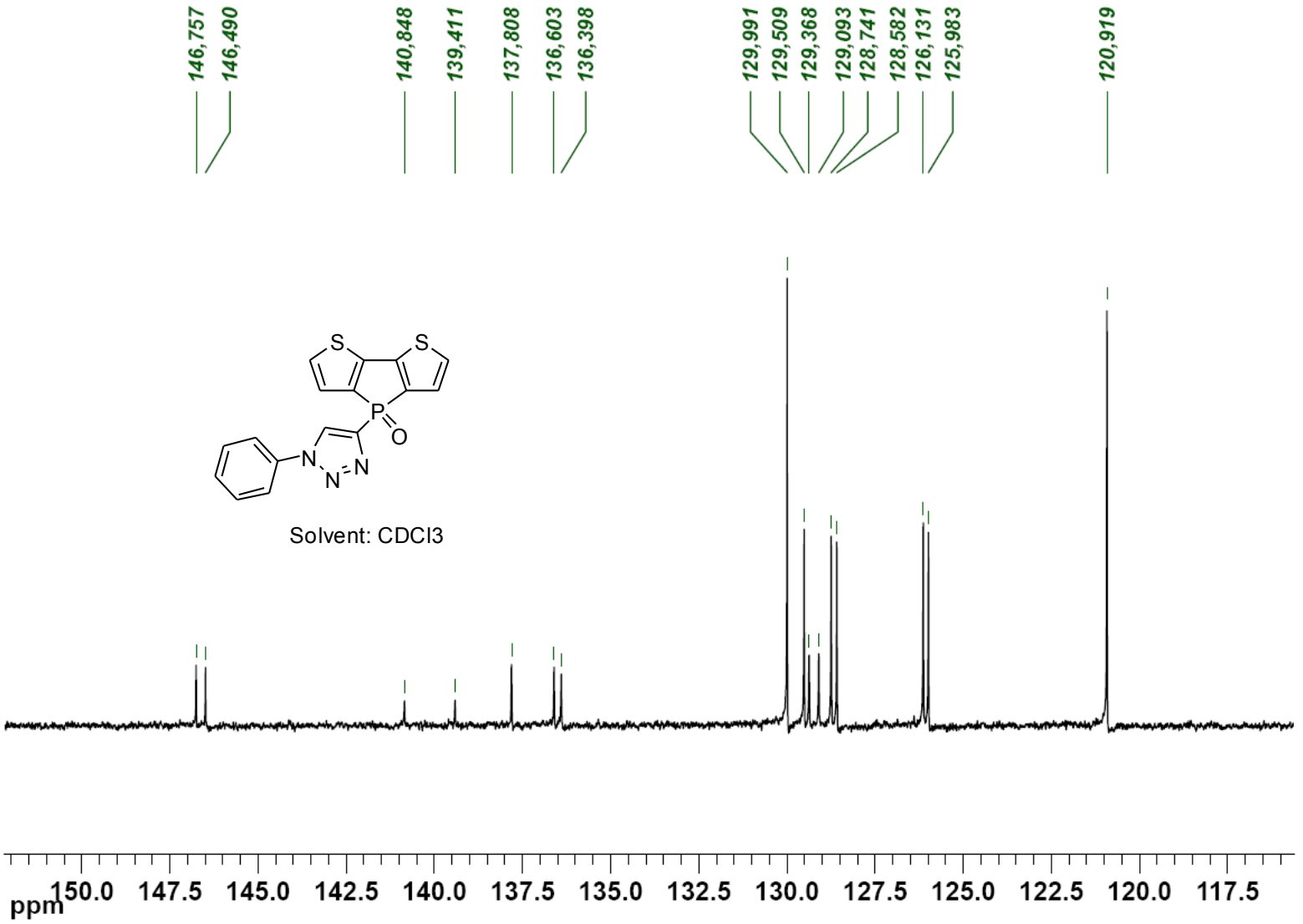

^{13}C NMR of **1** in $CDCl_3$

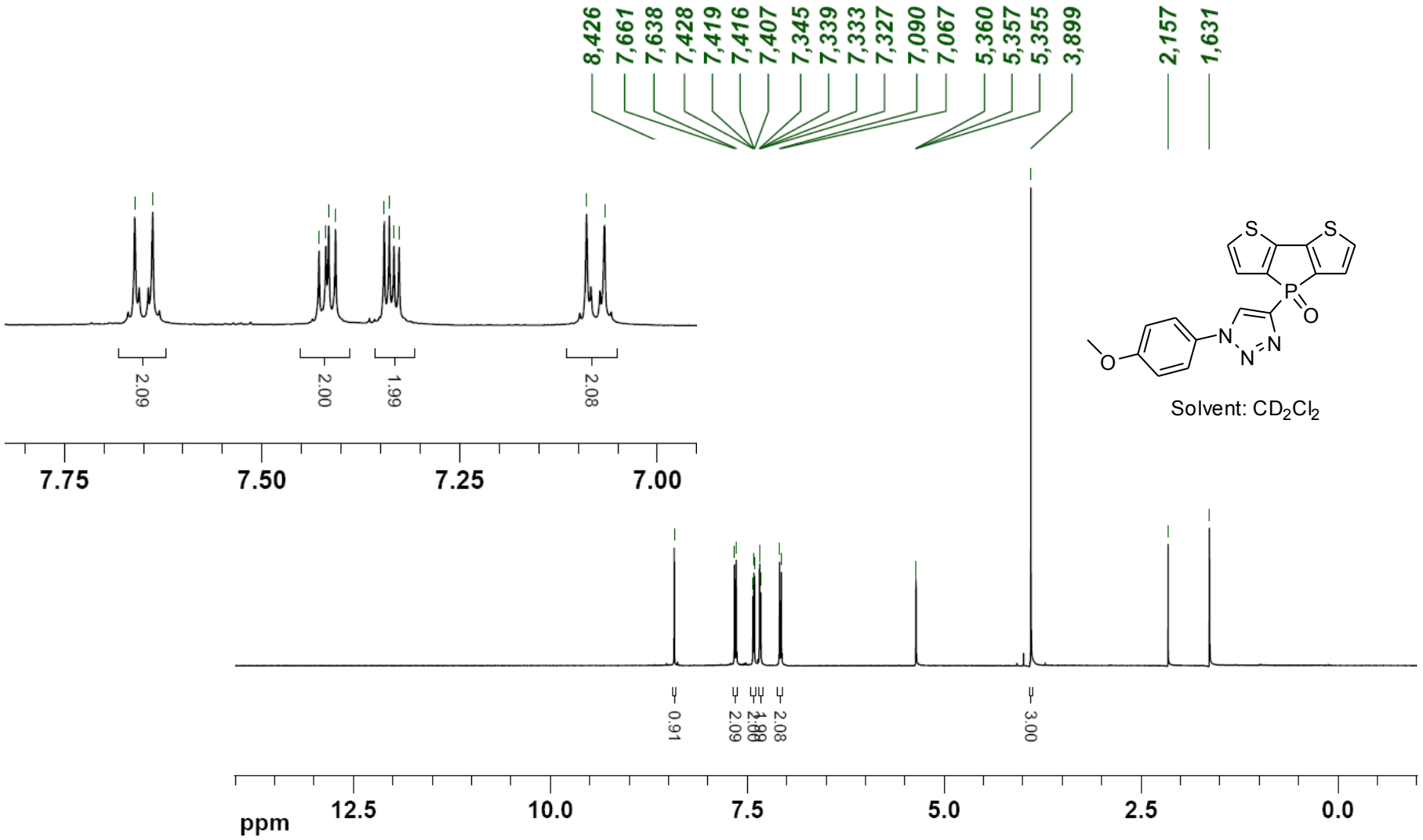

^{1}H NMR of **2** in CD_2Cl_2

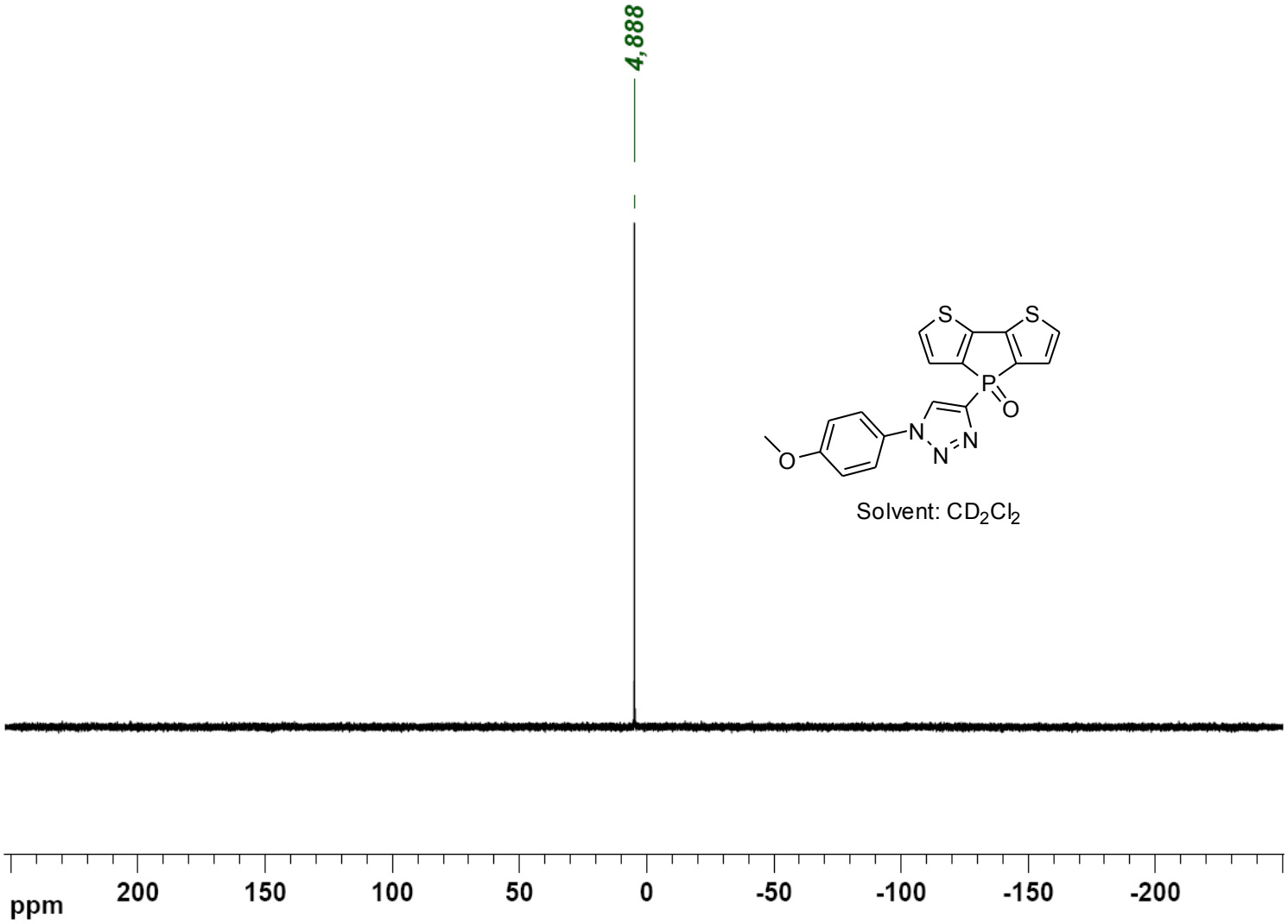

^{31}P NMR of **2** in CD_2Cl_2

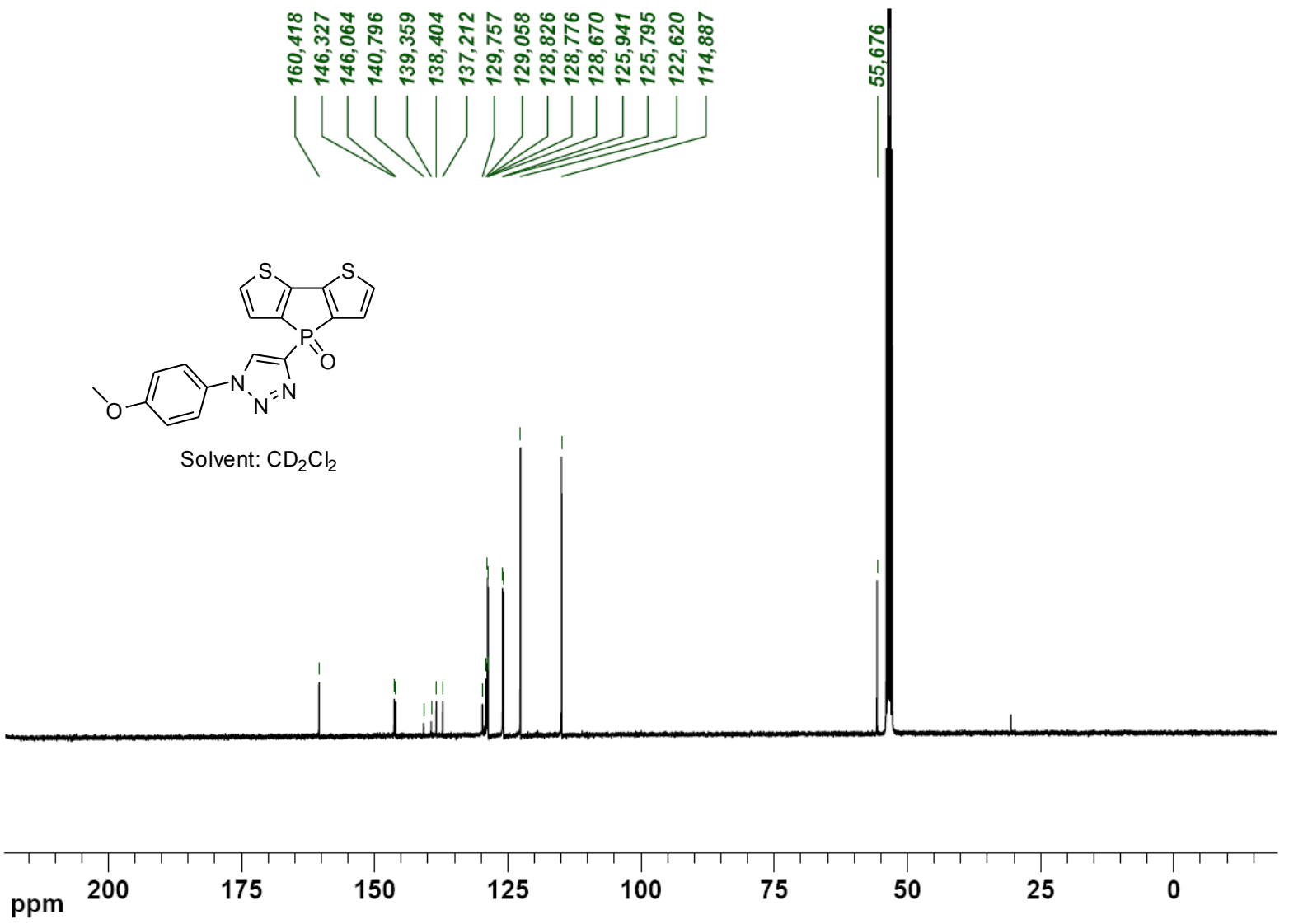

^{13}C NMR of **2** in CD_2Cl_2

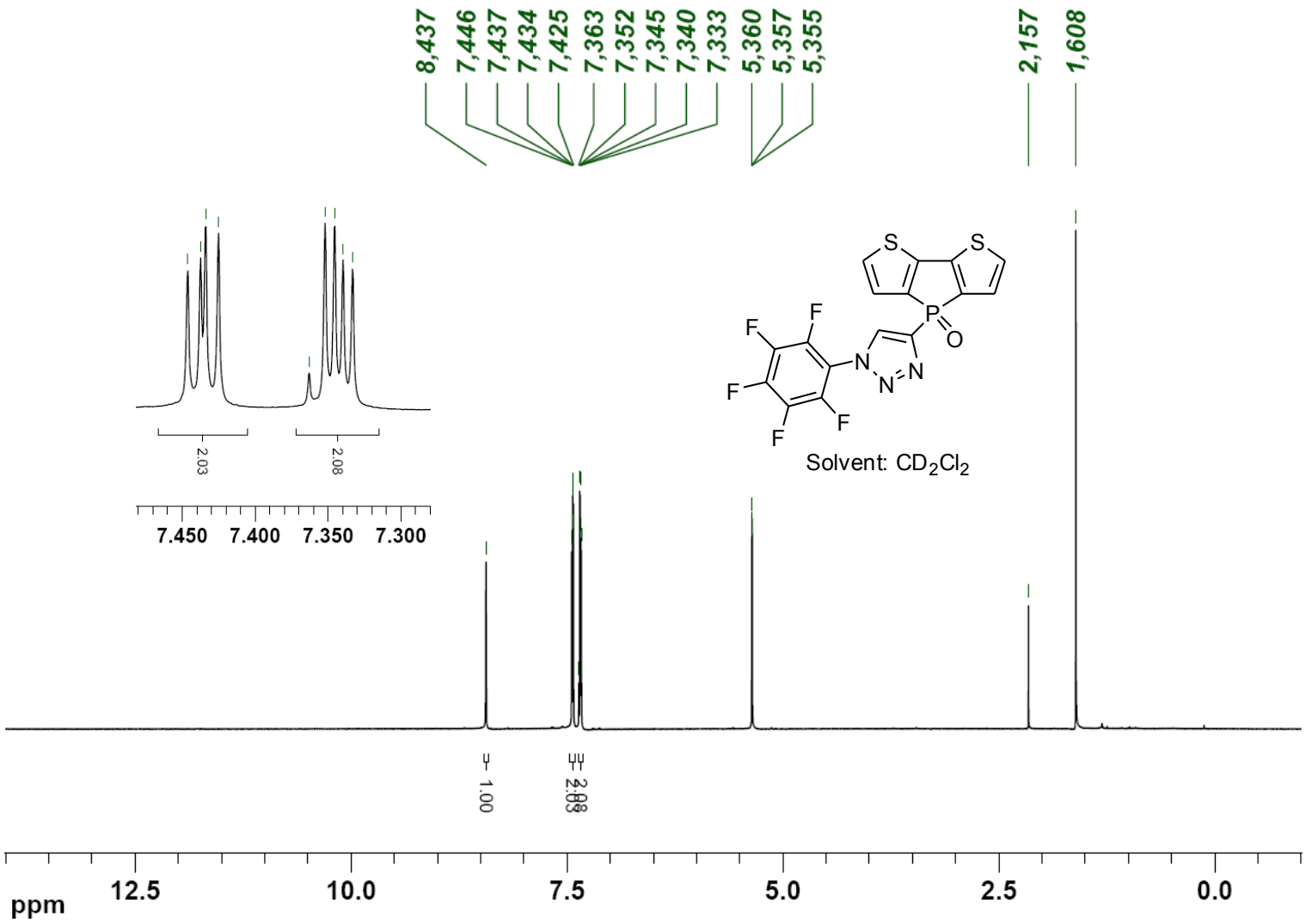

^{1}H NMR of **3** in CD_2Cl_2

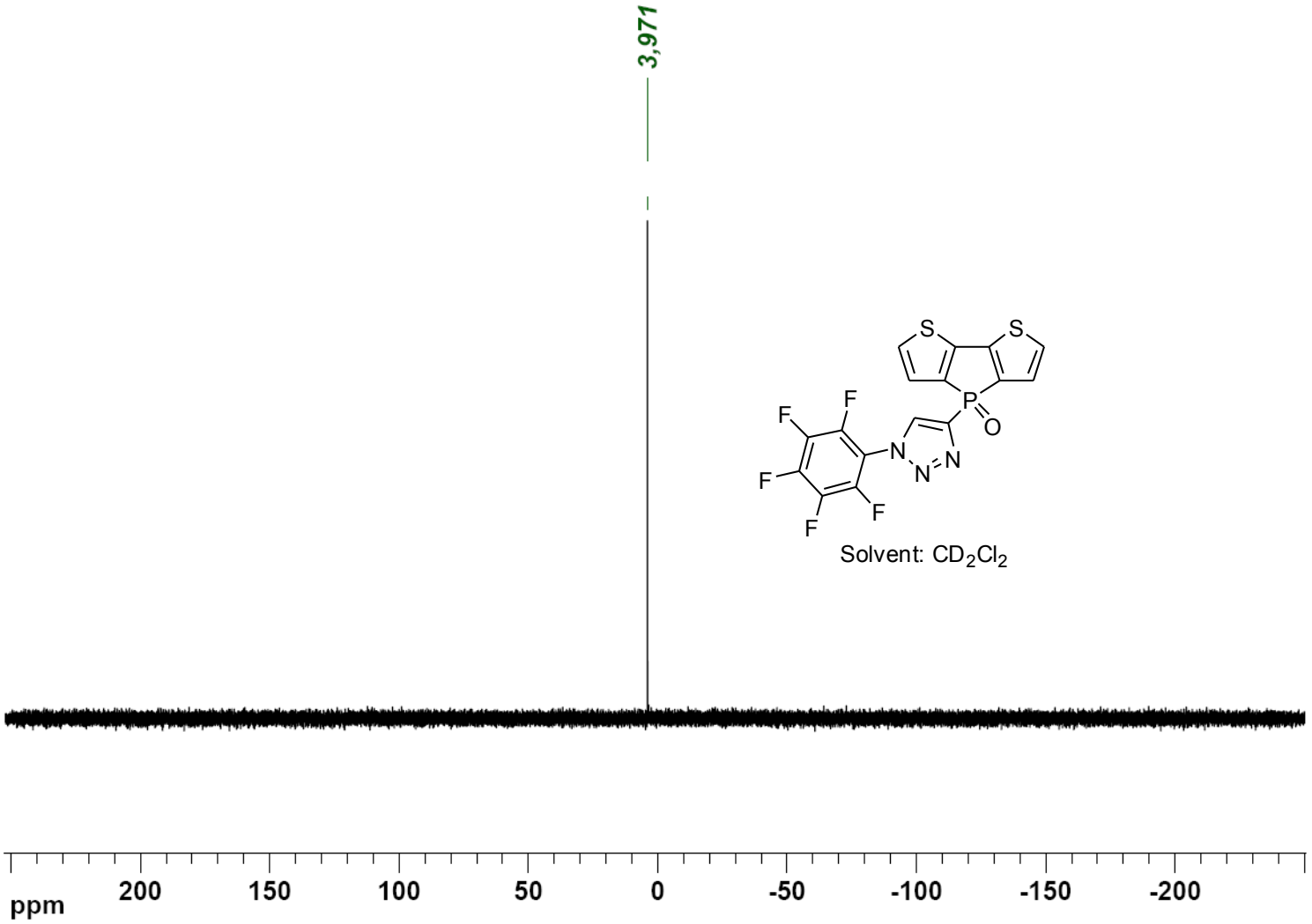

^{31}P NMR of **3** in CD_2Cl_2

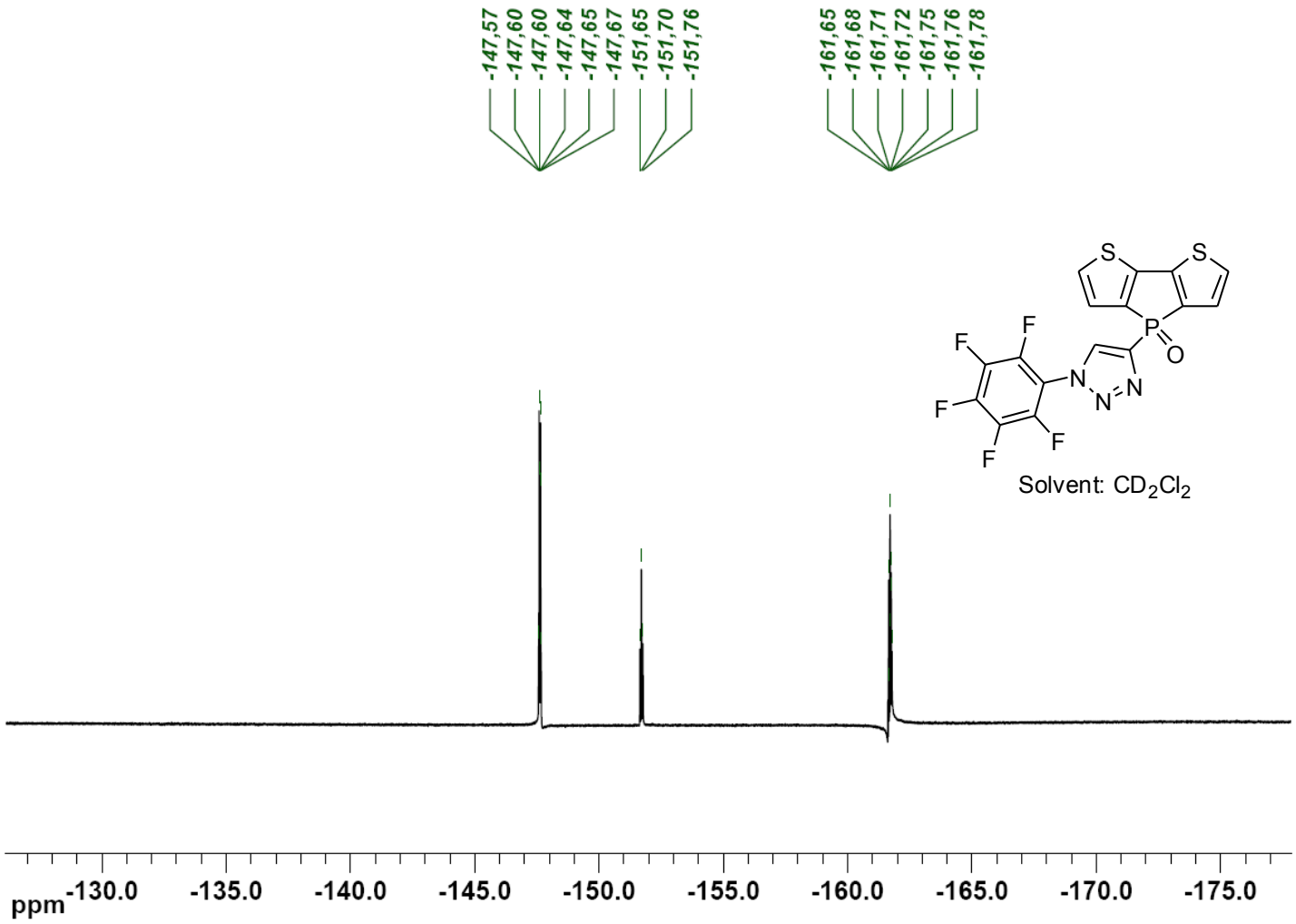

^{19}F NMR of **3** in CD_2Cl_2

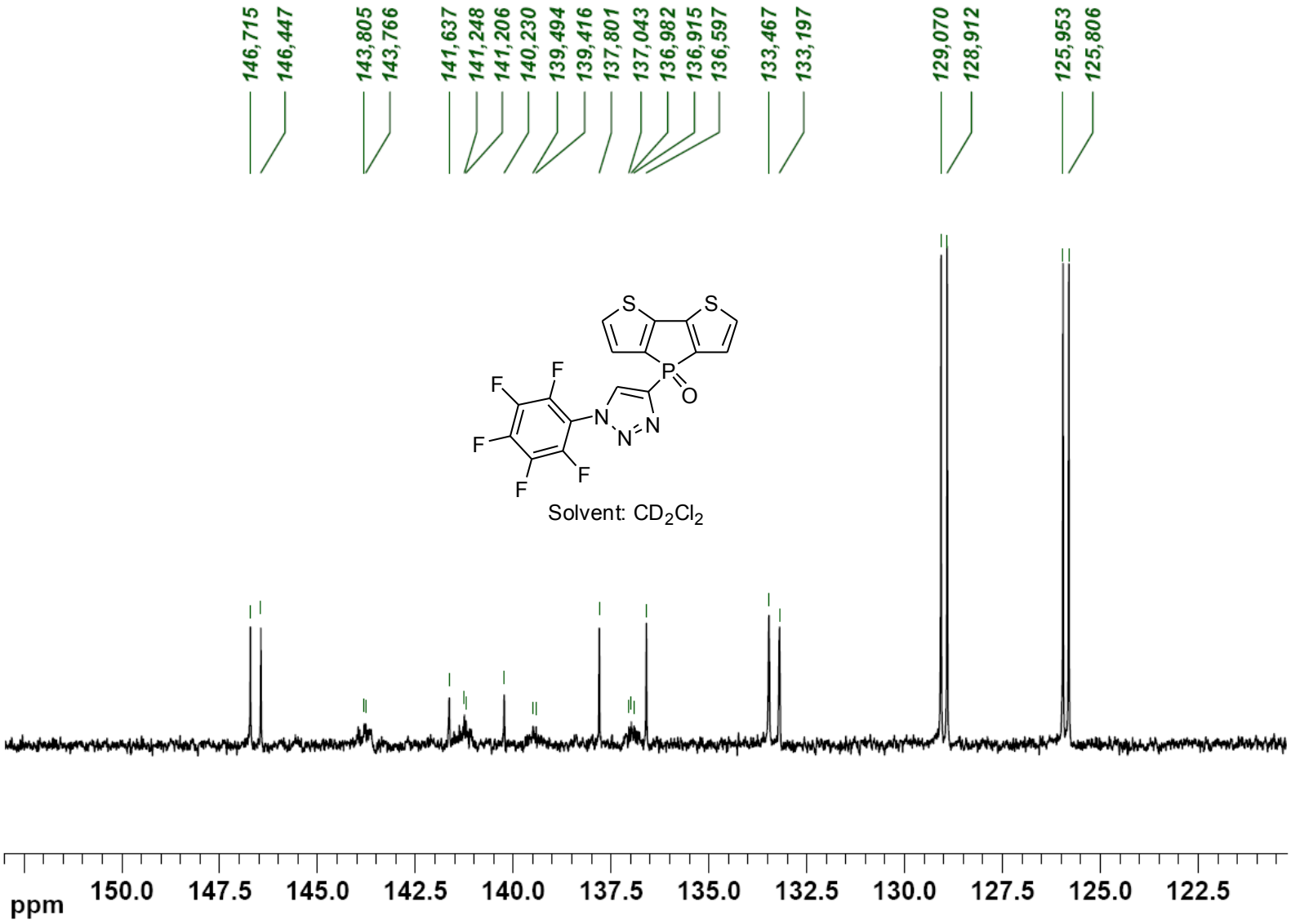

^{13}C NMR of **3** in CD_2Cl_2

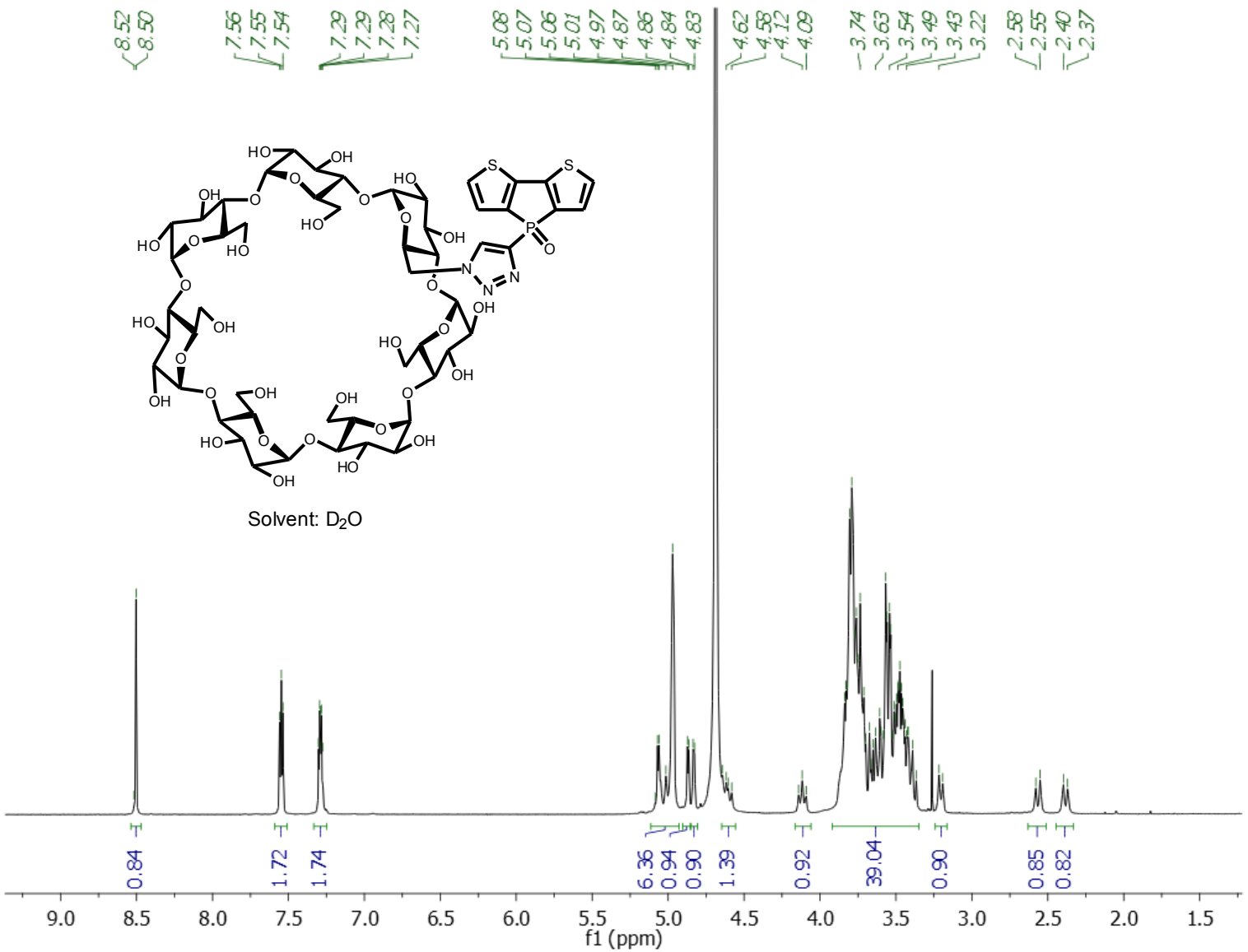

^{1}H NMR of **4** in D_2O

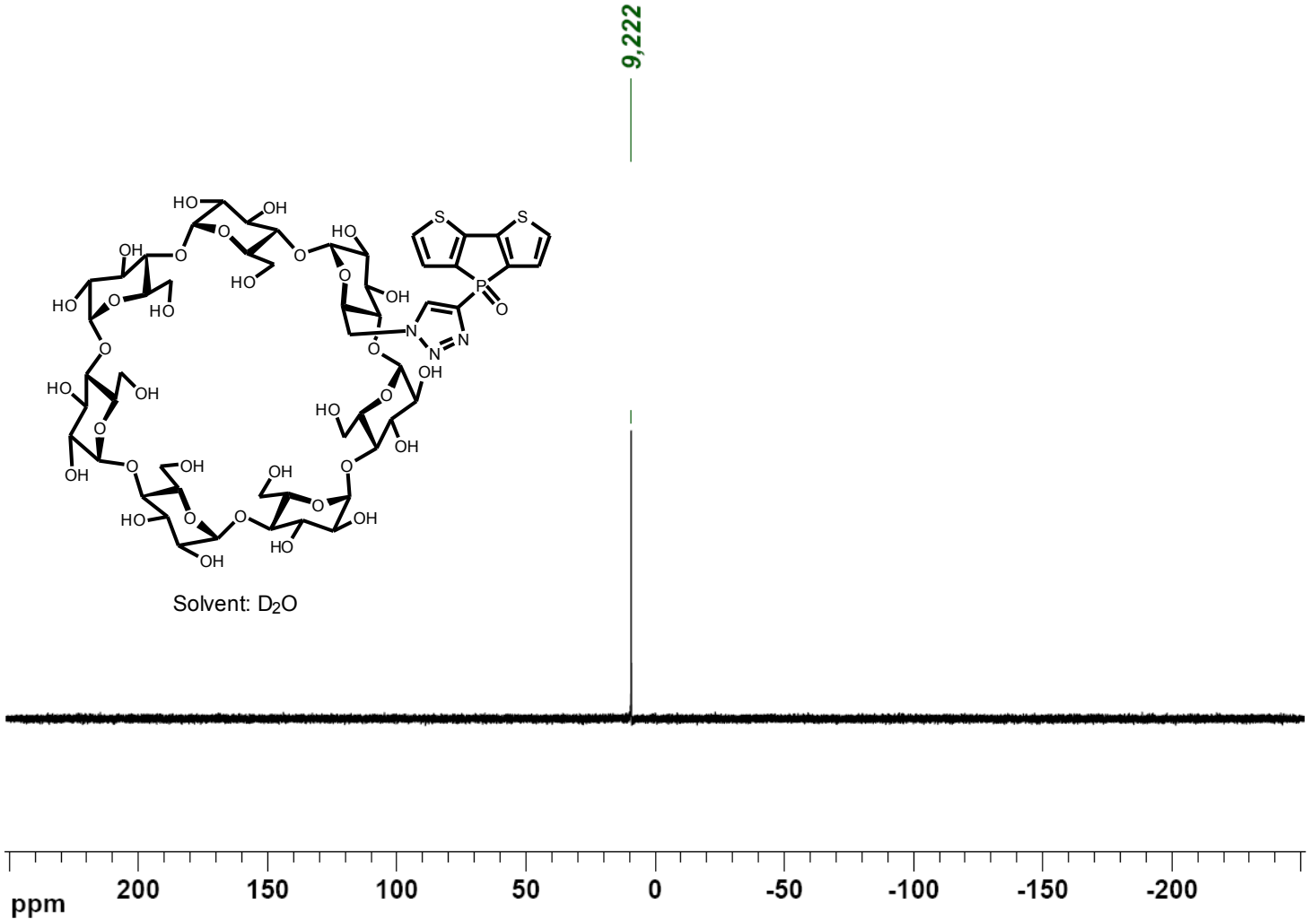

^{31}P NMR of **4** in D_2O

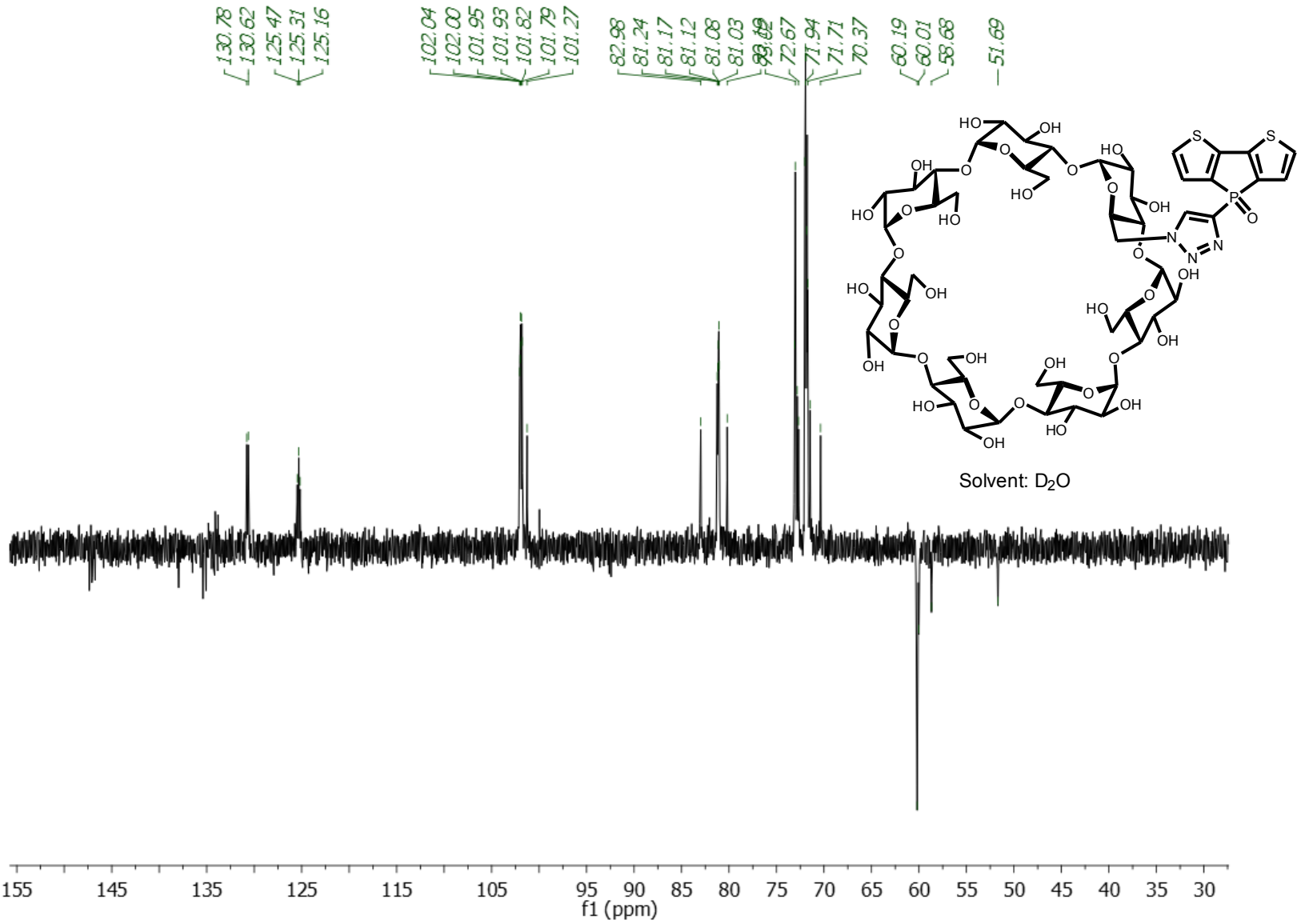

^{13}C NMR of **4** in D_2O

Computational Data

1. Optimized structure coordinates of **1**

C	-3.21155	-0.80851	-0.98559
C	-1.30365	0.33897	-0.3964
C	-0.85784	-0.96152	-0.1825
S	-2.1485	-2.12906	-0.41084
H	-4.18001	-0.95755	-1.41543
C	0.65111	-1.04444	0.21007
C	1.27548	0.19724	0.27459
S	1.76244	-2.34397	0.60664
C	3.09994	-1.15533	0.65643
H	4.13409	-1.41442	0.74759
P	0.0545	1.48045	-0.06846
O	0.41153	2.32343	-1.26275
C	-2.59894	0.46917	-0.80519
H	-3.08645	1.40492	-0.98295
C	2.61172	0.18283	0.55043
H	3.21727	1.05852	0.65705
C	-0.24486	2.61595	1.32202
C	-0.57857	2.27149	2.55936
N	-0.14697	4.07543	1.28423
H	-0.59878	1.27781	2.95568
C	-0.33823	3.51237	4.64164
C	0.95894	3.99738	4.8562
C	-1.09771	3.04147	5.72116
C	1.49663	4.01149	6.15027
H	1.53883	4.35692	4.03196
C	-0.56003	3.05558	7.01523
H	-2.08813	2.67115	5.55734
C	0.73714	3.54059	7.22978
H	2.48705	4.3818	6.31408
H	-1.13992	2.69603	7.83946
H	1.14768	3.55136	8.21783
N	-0.36257	4.50875	2.44341
N	-0.90223	3.49757	3.28422

2. Optimized structure coordinates of **2**

C	-3.29572	-1.95372	-2.03558
C	-2.10338	-1.02138	-0.29978
C	-2.62788	0.13917	-0.85995
S	-3.50887	-0.20254	-2.3392
H	-3.77042	-2.72653	-2.60332
C	-2.29317	1.42851	-0.0454
C	-1.5313	1.18238	1.09247
S	-2.64138	3.13921	-0.22802
C	-1.89576	3.43921	1.37145
H	-1.92625	4.37756	1.88475
P	-1.15144	-0.57975	1.16782
O	-1.66765	-1.2365	2.41948
C	-2.41789	-2.18818	-0.93343
H	-2.06627	-3.15341	-0.6341
C	-1.2621	2.26413	1.87935
H	-0.66803	2.23288	2.76873
C	0.62321	-0.96585	1.04976
C	1.61768	-0.08768	1.02025
N	1.21411	-2.30111	0.95482
H	1.52124	0.97454	0.93489
C	3.89305	-0.33651	0.18705
C	5.25146	-0.48494	0.49788
C	3.5119	0.28902	-1.00767
C	6.22872	-0.00784	-0.38602
H	5.54248	-0.96255	1.41007
C	4.48915	0.76613	-1.89156
H	2.47472	0.40235	-1.24499
C	5.84756	0.6177	-1.58073
H	7.26589	-0.12116	-0.14869
H	4.19813	1.24373	-2.80375
N	2.45667	-2.16724	0.82801
N	2.86796	-0.83697	1.11421
O	6.84476	1.10454	-2.48266
C	8.02071	0.29824	-2.37347
H	8.76687	0.66252	-3.04834
H	8.39304	0.34441	-1.3714
H	7.78214	-0.71552	-2.61896

3. Optimized structure coordinates of **3**

C	-3.45186	-2.62184	-1.29877
C	-2.2606	-1.29656	0.17666
C	-2.90052	-0.32059	-0.56794
S	-3.90657	-1.01062	-1.79619
H	-3.87014	-3.47363	-1.81802
C	-2.59542	1.0438	-0.17473
C	-1.70498	1.16093	0.87935
S	-3.14281	2.59131	-0.72548
C	-2.16874	3.39665	0.47897
H	-2.18745	4.47638	0.54202
P	-1.20651	-0.50675	1.44107
O	-1.39003	-0.86095	2.88315
C	-2.57309	-2.61636	-0.24718
H	-2.16872	-3.51556	0.20226
C	-1.46932	2.51147	1.25831
H	-0.82881	2.81924	2.07774
C	0.4808	-0.72035	0.8127
C	1.47535	0.20441	0.57094
N	0.99127	-1.96923	0.55716
H	1.50517	1.27794	0.66497
C	3.84823	-0.10027	-0.19996
C	4.93961	-0.9432	0.02841
C	4.02186	1.15288	-0.79348
C	6.214	-0.51816	-0.34133
C	5.30509	1.57079	-1.14423
C	6.40294	0.73848	-0.92109
N	2.22524	-1.86211	0.17612
N	2.54501	-0.53317	0.1786
F	7.64236	1.14518	-1.26886
F	5.47449	2.78134	-1.71728
F	2.95529	1.93946	-1.05082
F	4.73784	-2.14996	0.59896
F	7.27046	-1.32996	-0.12367

Full reference from main manuscript

(17) Frisch, M. J.; Trucks, G. W.; Schlegel, H. B.; Scuseria, G. E.; Robb, M. A.; Cheeseman, J. R.; Scalmani, G.; Barone, V.; Mennucci, B.; Petersson, G. A.; Nakatsuji, H.; Caricato, M.; Li, X.; Hratchian, H. P.; Izmaylov, A. F.; Bloino, J.; Zheng, G.; Sonnenberg, J. L.; Hada, M.; Ehara, M.; Toyota, K.; Fukuda, R.; Hasegawa, J.; Ishida, M.; Nakajima, T.; Honda, Y.; Kitao, O.; Nakai, H.; Vreven, T.; Montgomery, J. A., Jr.; Peralta, J. E.; Ogliaro, F.; Bearpark, M.; Heyd, J. J.; Brothers, E.; Kudin, K. N.; Staroverov, V. N.; Kobayashi, R.; Normand, J.; Raghavachari, K.; Rendell, A.; Burant, J. C.; Iyengar, S. S.; Tomasi, J.; Cossi, M.; Rega, N.; Millam, J. M.; Klene, M.; Knox, J. E.; Cross, J. B.; Bakken, V.; Adamo, C.; Jaramillo, J.; Gomperts, R.; Stratmann, R. E.; Yazyev, O.; Austin, A. J.; Cammi, R.; Pomelli, C.; Ochterski, J. W.; Martin, R. L.; Morokuma, K.; Zakrzewski, V. G.; Voth, G. A.; Salvador, P.; Dannenberg, J. J.; Dapprich, S.; Daniels, A. D.; Farkas, Ö.; Foresman, J. B.; Ortiz, J. V.; Cioslowski, J.; Fox, D. J. Gaussian09, Revision A.02, Gaussian, Inc.: Wallingford CT, 2009.